A New Approach to 3-D Ray Tracing for Propagation Prediction in Cities

George Liang, *Member, IEEE,* and Henry L. Bertoni, *Fellow, IEEE*

***Abstract*—A vertical-plane-launch (VPL) technique for approximating a full three dimensional (3-D) site-specific ray trace to predict propagation effects in cities for frequencies in the 300-MHz–3-GHz band is described and its predictions are compared with measurements for Rosslyn, VA. The VPL technique employs the standard shoot and bounce method in the horizontal plane while using a deterministic approach to find the vertical displacement of the unfolded ray paths. This approximation is valid since buildings walls are almost always vertical. The VPL method shows significant improvement compared with the slant-plane/vertical-plane (SP/VP) method for rooftop antennas. For a base station located at street level, the VPL method gives better predictions than the two-dimensional (2-D) method in locations where propagation over buildings is significant.**

***Index Terms*—Geometrical optics, propagation, urban areas.**

I. Introduction

RECENTLY, there has been considerable interest in using ray-tracing techniques together with the uniform theory of diffraction (UTD) to predict propagation within urban environments for frequencies in the UHF band. This interest is sparked by the growth of wireless communications and the introduction of personal communication services (PCS), which requires the use of microcells covering ranges of less than 1 km to support the anticipated high density of users. Over these small ranges, statistical prediction models based on measurements can show considerable error, especially in areas having mixed building sizes. In contrast, ray-tracing techniques that are able to find the dominant propagation paths can be expected to exhibit accuracy and efficiency over these small ranges, thus providing a theoretical model that is superior to the statistical models.

The key to any robust ray-tracing propagation model is to find a computationally fast way to determine the dominant ray paths so as to provide accurate path-loss predictions. It is well known for outdoor propagation prediction that in addition to specular reflections, diffraction at edges must be accounted for, especially in nonLOS regions. Unfortunately, diffractions are very inefficient to model since a single source ray at an edge will generate a whole family of new rays [1]. The generation of so many diffracted rays limits the number of diffractions that can be considered on any given ray path to at most two, unless an approximation can be made to find the few contributing rays. Such an approximation is essential for some building environment since the dominant paths involve multiple forward diffraction over many buildings [2].

In order to find the contributing rays in an urban environment wherein building walls are nearly always vertical planar polygons, we have developed the vertical-plane-launch (VPL) method. The VPL approach accounts for specular reflections from vertical surfaces and diffraction at vertical edges and approximates diffraction at a horizontal edges by restricting the diffracted rays to lie in the plane of incidence, or in the plane of reflection. Compared to the full three-dimensional (3-D) shoot and bounce ray (SBR) method [3] or the 3-D image method [4], that can handle at most one or two diffractions for any edge orientation, the VPL approach can treat many multiple forward diffraction at horizontal edges. Unlike the vertical-plane/slant-plane (SP/VP) approximation [5] whose application is limited to low base-station antennas, the VPL method can be used for rooftop antennas and areas of mixed building heights. It provides nearly identical results with the two-dimensional (2-D) method for low transmitting and receiving antennas in a tall building environment, in which case propagation takes place around buildings. The predictions of the VPL method are in good agreement with the measurements made in Rosslyn, VA.

II. Vertical-Plane-Launch Method

The concept of the VPL method for a rooftop antenna is indicated in Fig. 1, which shows half planes originating from a vertical line through the transmitter and extending outward in one direction. As an example, the plane labeled “1” extending between the transmitter and receiver 1 in Fig. 1 contains a ray that must propagate over the intervening rows of building. The ray reaching receiver 2 consists of two segments with the incident ray contained in vertical plane 1 and the reflected ray is contained in plane 2 representing a reflection from the tall building then traveling over a series of lower buildings before arriving at the receiver. For receiver 3, the illuminating ray in the vertical plane 3 must undergoes diffraction at the vertical edges of two buildings before traveling over the rooftops of lower buildings to the receiver.

Unlike a full 3-D SBR method, where rays are launched in 3-D space and all directions are treated in a unified manner, the VPL method takes into account the nearly universal use of vertical walls in building construction and differentiates the horizontal and vertical directions. In the horizontal directions, 2-D rays representing the vertical planes are launched from the source in a manner similar to that of the 2-D pin-cushion method previously used for indoor propagation [6]. This method generates a binary tree at the point where the

Manuscript received March 18, 1997; revised January 12, 1998.

The authors are with the Center for Advanced Technology in Telecommunications, Polytechnic University, Brooklyn, NY 11201 USA.

Publisher Item Identifier S 0018-926X(98)04874-1.

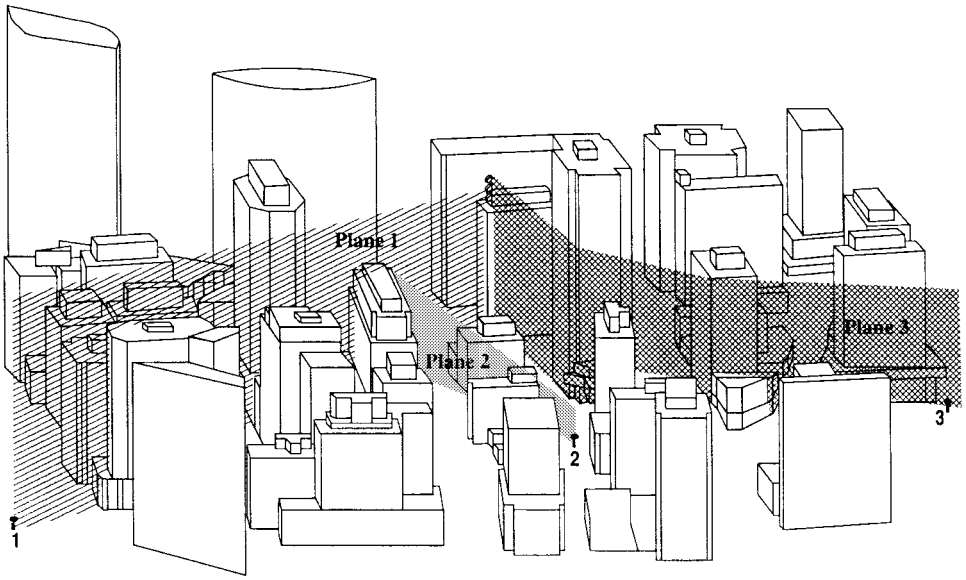

Fig. 1. Approximate 3-D ray-tracing method using vertical planes.

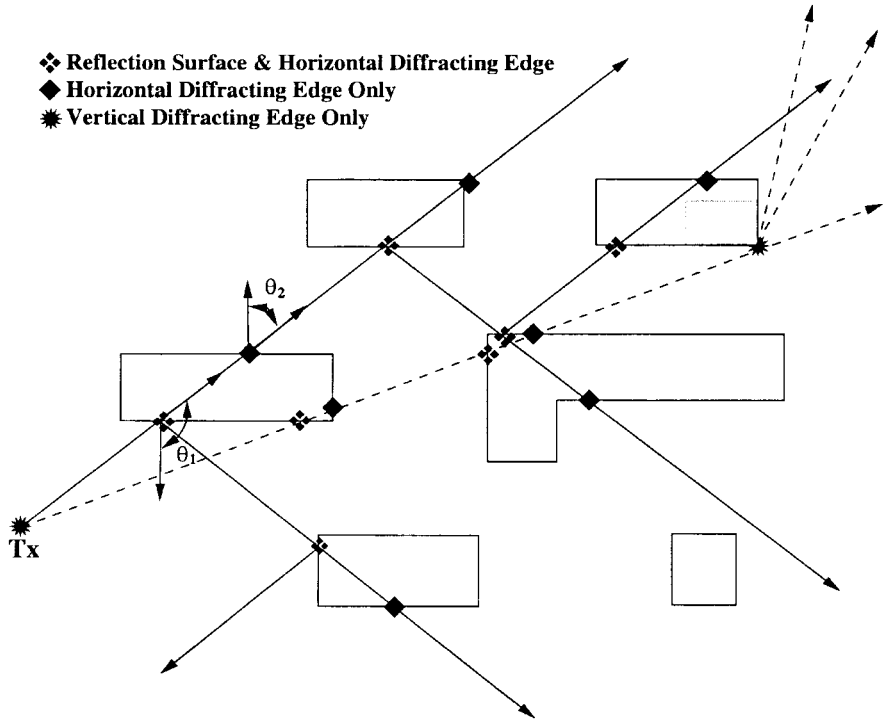

Fig. 2. Rays generated from the VPL method in the horizontal plane.

vertical plane intersects an exterior face of a building wall, with one plane continuing along the incident direction and a second plane going off in the direction of specular reflection, as shown in Fig. 2. The plane that continues in the incident direction contains rays that propagate directly over the building and rays that are diffracted over the buildings at its horizontal edges. The plane that is spawned in the reflected direction contains rays that are either specularly reflected from the building face or are diffracted at the top horizontal edge of the wall. The path that a ray travels in the vertical direction is found by examining the profile of all the buildings in the unfolded set of vertical plane segments between the source and receiver and uses deterministic equations to calculate the vertical displacement and received signal strength.

A vertical plane segment is considered to have illuminated the receiver if two conditions are met. The ray must intersect the capture circle of a receiver, as described in [6] and it must lie in the vertical wedge of the illumination. The capture circle is a concept used in conjunction with rays traced at a discrete angular separation to ensure that the signal associated with a continuous family of rays undergoing the same set of reflections and diffractions before illuminating the receiver is

counted once and only once. In the vertical plane the illumination wedge is used to represent the extent in the vertical direction of the region illuminated by a continuous family of rays that have undergone a particular set of reflections and diffractions.

Once the receiver is considered to be illuminated then all the interactions along the unfolded path can be use to determine the total path loss. In addition to the path length effects, the total path loss depends on the product of the reflection and diffraction coefficients. For a vertically or horizontally polarized source, the reflection coefficient at walls is approximated by that of a TE- or TM-polarized plane wave, respectively, at a dielectric half space [7] with a dielectric constant of $\epsilon_r = 6$. The use of the reflection coefficient for a dielectric half space with $\epsilon_r \approx 5$–7 is suggested by direct measurements [8], and this range of ϵ_r is found in our predictions to give the least error with the measurements. Diffraction at edges can be approximated as the product of the UTD diffraction coefficients from an absorbing [9], perfectly conducting [10], or dielectric wedge [11] although this is limited to a few edges in cascade. Alternatively, numerical techniques such as discussed in [12]–[14] can be employed when more than a few horizontal edges must be accounted for, as discussed below.

The ray-trace architecture is describe by the flow chart shown in Fig. 3 and contains three major modules. One module contains the functionalities used to determine if a vertical plane will intersect with the walls of the building. The second module determines whether a receiver will be illuminated by the vertical plane and, if so, calculates the path loss associated with this path. Finally, the third major component finds all the vertical building corners that will be illuminated by the vertical planes and stores the information necessary to subsequently determine the diffracted field at a receiver. The ray trace utilizes these three modules in a recursive and repetitive manner for each plane emitted from a source.

The VPL technique is able to account for rays that undergo multiple interactions as a result of a combination of forward diffractions at horizontal edges with reflections from building walls and single or double diffraction at a vertical edge of a building. The VPL method neglects rays that are transmitted through the building, diffuse scattering from the walls, and rays that travel under a structure. It also neglects reflections from the rooftop, which travel upward and, hence, away from the buildings and receivers. These simplifications are made because it is believed that the rays do not significantly contribute to the total received power in a microcellular environment or that they occur very infrequently and their inclusion would substantially increase the model's complexity and the computation time.

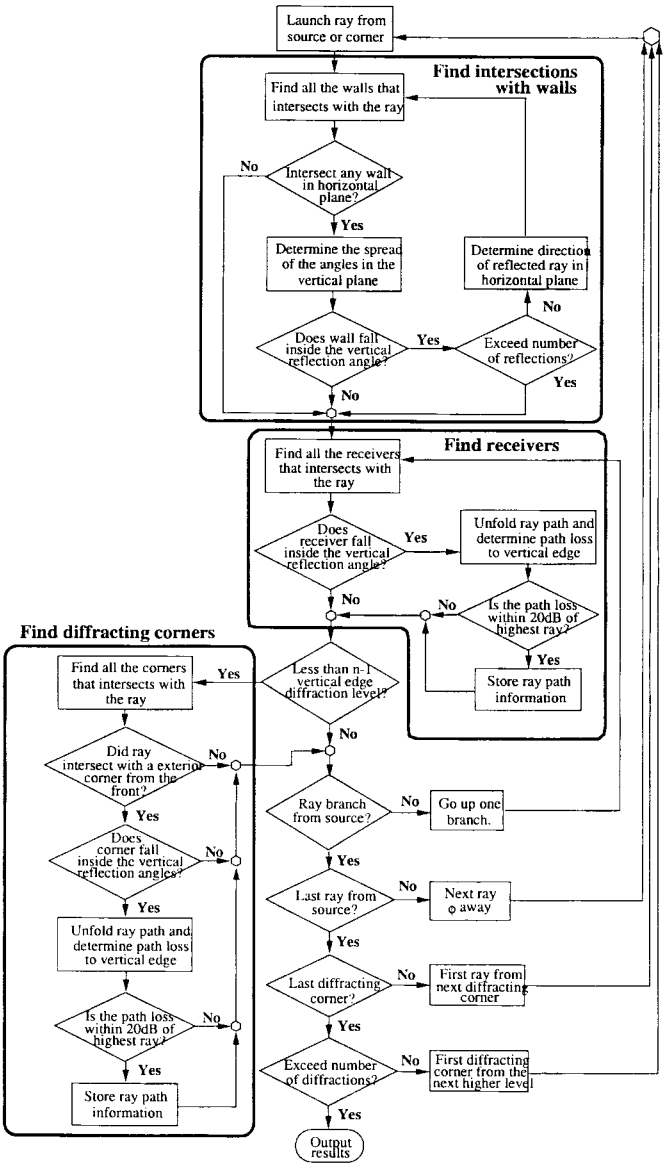

Fig. 3. Flow chart of the VPL method.

A. Description of Building Database for Ray Tracing

Since ray launching is confined to the horizontal plane, the buildings are represented by their footprints as closed polygons. A simple building may consist of an arbitrary number of points representing the vertical edges of the building and ordered in a counterclockwise direction. Instead of representing each surface of the building explicitly, this method allows for a simpler representation by assuming the walls are vertical. The vertical dimensions and locations of the building relative to a datum point are explicitly retained in the database. Buildings that are comprised of multiple stacked structures are represented by an equal number of separate polygons that overlap each other. Buildings with simple slanted roofs can be represented by including a larger vertical dimension at the higher vertices. By combining two slanting roofs, peaked roofs can also be represented as two structures coupled together along the line forming the apex of the roof. While reflection from the roofs is neglected, by including slanting roofs we are able to more accurately model diffraction over such buildings.

B. Reflection from Vertical Walls

Reflections from building walls are considered to be possible if the angle θ, between the incident 2-D ray representing the vertical plane and the outward normal of the wall in the

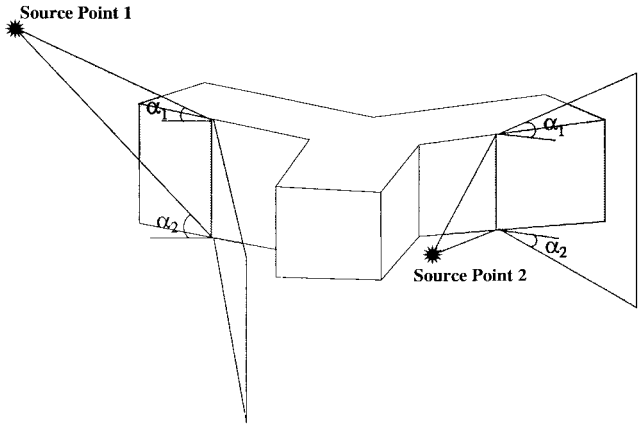

Fig. 4. Creation of wedge sector due to reflection from wall.

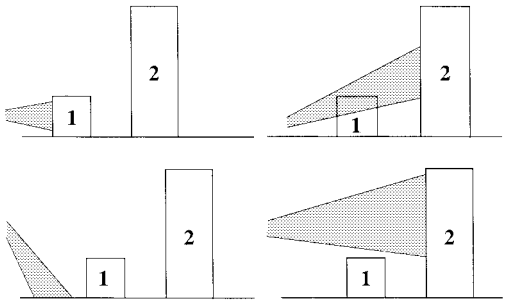

Fig. 5. Test of reflection sectors in the vertical plane.

horizontal plane is greater than 90°. The angle θ_1 in Fig. 2 represents the case when a reflection from the building wall is possible while θ_2 indicates the case when it is not. In general, when a 2-D ray passes through a polygon representing a building there will be at least one reflecting and one nonreflecting surface. For the case when a building is comprised of multiple stacked structures represented by nested polygons there is a reflected 2-D ray generated by each surface whose outward normal makes an angle of greater than 90° with the incident 2-D ray. In the vertical plane, reflections are consider to be possible if the vertical extent of the ray family represented by the plane overlaps the vertical height of the wall. The initial plane from a source is of infinite extent in the vertical (z) direction but, after the first reflection, its extent will be limited by the angles between the source and the top (α_1) and bottom (α_2) edges of the reflecting wall (as shown in Fig. 4).

If the source is higher than the top edge of a reflecting surface (as for source point 1 in Fig. 4), then both α_1 and α_2 are negative, while if the source is below the top edge (as for source point 2), then $\alpha_1 > 0$ but $\alpha_2 < 0$. An additional case not shown in Fig. 4 is when both α_1 and $\alpha_2 > 0$ as a result of the source being below the bottom of the wall. These wedge-shaped sectors give the limits in the reflected vertical plane of the geometrically reflected fields and are tracked through subsequent building interactions to determine the region illuminated by the reflected rays. Outside of the wedge sector, rays that are back diffracted from the top edge of the wall give a dominant contribution to the field in the reflected vertical plane segment. The procedure used to keep track of the regions in which the back diffracted rays contribute through subsequent building interactions is discussed below.

The major computational effort in the program is to determine the intersection points of the vertical plane segments with the building walls. Because a binary tree is created by the reflected vertical planes, allowing for N reflections generates $\sum_{n=0}^{N} 2^n$ plane-wall intersections that must be computed for each initial vertical plane. In order to reduce the number of such computations, a pruning procedure based on α_1 and α_2 is used to terminate the tracing along certain branches, as suggested in Fig. 5. An additional restriction is imposed by limiting the number of back diffraction from horizontal building edges to a single event.

Fig. 5 shows several different cases for a wedge-shaped sector that can occur when testing the illumination wedge in the vertical plane. When the wedge illuminates the face but the not the top edge of building 1 as shown in Fig. 5(a), the vertical plane segment in the reflected direction is continued while the vertical plane segment in the incident direction is terminated. The most general case when no pruning of the ray occurs is shown in Fig. 5(b), where the wedge of rays illuminates the face and the top edge of building one. In this case, the transmitted vertical plane continues to building 2 in the incident direction, and a specular reflected vertical plane is created at building one. For the case shown in Fig. 5(c) the opposite is true—neither the transmitted nor reflected vertical planes are generated because the wedge fails to intersect the wall. Finally, in Fig. 5(d) the vertical plane that is transmitted past building one is continued to the next building, while no reflected plane is created at building one.

C. Multiple Diffraction at Horizontal Edges

The continuation of the incident plane past a building is used to represent rays propagating over the buildings and to approximate rays diffracted by the horizontal edges. A list of building walls intersected by the vertical plane segments is created for each vertical plane segment that begins from a source or is spawned from a reflection. When the final vertical plane segment illuminates a receiver point, the entire series of horizontal building edges lying between the source and receiver is available in the unfolded vertical plane. Since not every edge that intersects the vertical plane interacts with the ray reaching a receiver location, only those edges that influence the ray field need to be found in order to determine the diffraction loss due to propagation over the buildings. The significant edges can be described by the concept of the convex hull, which finds the set of points that forms the smallest polygon for which each point in the set is either in the boundary of the convex polygon or in its interior. The convex hull can be thought of as the shape of a rubber band going around the edges and ending on the source and receiver points. For diffraction over buildings, it is only necessary to find the upper convex hull; that is, only those edges that protrude above an imaginary line connecting the source and receiver points. Note that the source and receiver locations are the end points of the convex hull.

A profile of all horizontal edges is initially constructed from the unfolded vertical plane between the transmitter and

receiver. The algorithm then removes all edges that are below the line between the source point $p' = (x', z')$ and prediction point $p = (x, z)$ and from the remaining points, if any, finds all the edges that form the largest convex perimeter of edges. These edges are designated as diffracting edges that block the ray from traveling directly between the source and the receiver.

Within each segment between these convex hull points there can be additional edges that might interfere with the propagation of the field if the edge lies in the Fresnel zone. In the vertical profile, the Fresnel zone is an elliptical region about the line joining two adjacent points in the convex hull that are at its foci. The half-width w of the Fresnel zone at any point between two convex hull can be approximated by

$$w \approx \sqrt{\frac{n\lambda s(l-s)}{l}} \tag{1}$$

where l is the length of the line connecting the two convex hull points, s is the distance along the connecting line measured from a convex hull point, λ is the wavelength, and n is the Fresnel zone number. The complete list of diffracting edges consists of the edges in the convex hull and any edges within the Fresnel zones connecting convex hull points. A Fresnel zone index $n = 0.5$ is adequate to account for all significant diffraction effects. In order to reduce the number of diffraction calculations associated with the Fresnel zone edges, only the edge that most significantly interfered with the Fresnel zone is used. The additional diffraction loss caused by the edge is obtained from the application of a simple formula for a nonobstructing knife edge [15].

The effect of diffracting past all of the significant edges can be determined from numerical integration [12], [14]. However, for the predictions reported here we have used a simplified procedure that is more computationally efficient. If the list of convex hull points has four or fewer edges, the UTD diffraction coefficients [11] for all the edges are cascaded. For more than four edges in the convex hull, a procedure is used to select the four edges used to approximate diffraction over the rooftops. This procedure retains the edge closest to the receiver and the one immediately after the transmitter. It then finds the two other edges falling in between that protrude the furthest above the line joining the source and receiver. If one of the edges in the convex hull is a back diffracting edge, then it must be retained and the other three edges are found by the procedure just outlined.

The VPL method will allow for a single-back diffraction from a horizontal edge anywhere along the ray path. If the top edge of a wall is illuminated, but the vertical wedge reflected from the wall fails to illuminate the top edge of the next wall then a back diffraction is considered to have occurred at the first edge. The back diffraction acts as a secondary source and is implicitly carried forward because the vertical wedge immediately after the back diffracting edge has an infinite extent in z once again. For this instance, the geometrical optic rays do not propagate over the rooftop but rather it is the diffracted rays that carry energy over the building. Since back diffraction is a comparatively weak propagation phenomenon, we allow for its inclusion only once along a ray path. The addition of a back diffraction edge is treated in a slightly different manner when performing the convex hull test and in calculating the path loss. Since the back diffracting edge must be included in the vertical profile of edges, it becomes necessary to perform two convex hull test, one in the segment of the unfolded vertical plane between the source and the back diffracting edge and the other in the segment between the edge and the receiver. In this way, all significant edges will be included in the excess loss calculations.

In Fig. 6 the unfolded vertical plane of a typical trace shows a ray path that has undergone a back diffraction along with diffraction over building rooftops and reflections from building walls. The vertical profile shown in Fig. 6 represent the unfolded path of five ray segments. Each segment or fold lines of the vertical plane in 3-D is delimited by a reflection (light dashed line), a back diffraction (dotted line), the source, or receiver. In this example there are six points in the convex hull including the source and receiver, which are the end points, and four horizontal edges where diffraction must occur in order for the signal to reach the receiver. The edges include the single-back diffracting edge as well as the two edge of the tall building and the edge just prior to the receiver. After all the convex hull edges have been found, edges that fall within the separate Fresnel zones between each pair of convex hull points are determined. In the example shown in Fig. 6, only the edge closest to the source (shown as a heavy dashed line) falls inside the $n = 0.5$ Fresnel zone.

D. Diffraction at Vertical Edges

Diffraction at vertical edges (corners) are treated in a manner similar to that of a 2-D ray trace in the horizontal plane, where building corners are represented by a point. Vertical plane segments that pass through the corner's capture circle are considered to have illuminated the corner and are stored as a series of source planes for that corner. The vertical edge is then treated as a secondary source of vertical planes, whose vertical extent is limited by the largest illumination wedge of all the source planes. Single-corner diffractions are the result of illumination from the source, which may illuminate the edge after one or more reflections and/or diffraction at horizontal edges, while double-corner diffraction is due to illumination from first-order corner-diffracted rays, again, after further possible reflections and diffractions at horizontal edges. An example of diffraction around the building is shown by the dashed rays in Fig. 2. The incident or source ray illuminates the corner after traveling over two buildings while the diffracted rays originate at the corner and are traced identically like the rays from the transmitter.

When a plane that is diffracted from a vertical edge illuminates a receiver point, the list of reflecting walls and horizontal edges for each vertical plane that illuminated the corner is attached to the list of horizontal edges between the corner and the receiver. The diffraction coefficient [11] for the corner is determined from the angles that the incident and diffracted vertical planes make with the normal to the illuminated wall. Then using the techniques described in the previous section, all the diffracting horizontal edges, if any, are found and their excess loss is calculated. Finally, the total path loss is

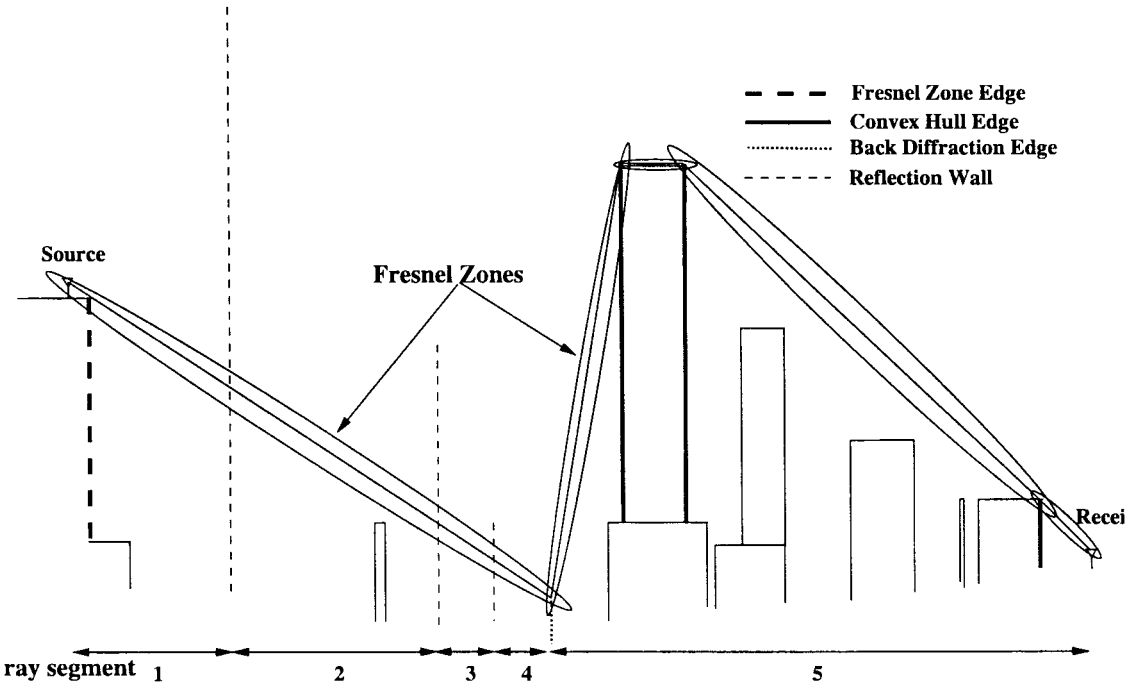

Fig. 6. Vertical profile of horizontal diffracting edges.

the sum of the free-space path loss and the excess path loss due to reflections, horizontal, and vertical edge diffractions. This procedure is performed once for each source ray that has illuminated the corner. For double-corner diffraction, all combinations of vertical planes from the source to the first corner from the first to the second corner and from the second corner to the receiver need to be used to find all possible ray paths.

E. Ground Reflection

A reflection from the ground is accounted for by assuming the ground is horizontal in the vicinity of the receiver. The two-ray model for paths within the same vertical plane is then used, taking the source in the two-ray model to be the closest point in the convex hull. The fields of the direct and ground reflected rays are added coherently to allow for their destructive interference at large distance. The ground reflected path r_b has a path length equal to the distance from the image source to the receiver. The length of the direct r_a and ground reflected rays r_b are given by

$$\begin{aligned} r_a &= \sqrt{(x-x')^2+(y-y')^2+(z-z')^2} \\ r_b &= \sqrt{(x-x')^2+(y-y')^2+\left(z+z'-2z_g\right)^2} \end{aligned} \tag{2}$$

where (x', y', z') and (x, y, z) are the coordinates for the closest point in the convex hull and the receiver point, respectively, and z_g is the height of the ground at the receiver. The effect of coherently summing the two rays can be approximated by the product of the direct ray signal and the factor $|(1-\Gamma_g e^{-jk(r_b-r_a)})|^2$ where Γ_g is the Fresnel reflection coefficient for a plane wave incident on a lossy dielectric half-space.

III. Predictions in an Urban Environment

Measurements were conducted by AT&T at 900 and 1900 MHz in the downtown core of Rosslyn, VA, which is comprised of a few lower buildings dispersed among mostly high-rise office buildings, as shown in Fig. 1. The building footprints, as well as the transmitter and receiver locations, are are shown in Fig. 7. The 400 receivers or prediction points are ordered consecutively for each street along the drive route and are located 5 m apart and approximately 2.5 m above the ground. Transmitters 5 and 6 are on rooftops at a curb height of 42 and 44 m, respectively, and both employ directional antennas (beamwidth 25–30°) with $Tx5$ directed along the positive y axis and $Tx6$ along the positive x axis in azimuth, while both are downtilted 6°. All other transmitters use an omnidirectional antenna at both frequencies and are located 10 m above street level.

The measurements were taken simultaneously for both frequencies and one second average of the signals were recorded at 1-m intervals as the measurement vehicle drove down each street. The measured path loss for each prediction points was determined from the average of all measurements points that were within a 5-m-diameter circle of the receiver in order to average out the fast fading of the signal. For comparison, we have predicted the sector averaged received power normalized over 1 W of transmitted power by summing the individual powers of the contributing rays [16], except for the use of the two-ray model to account for ground reflections.

A. Comparison with the Slant/Vertical Plane Method

For a rooftop transmitter, the dominated propagation mechanisms are expected to include paths that go over as well as around the buildings. This includes paths that travel over a series of buildings before diffracting at a horizontal edge down

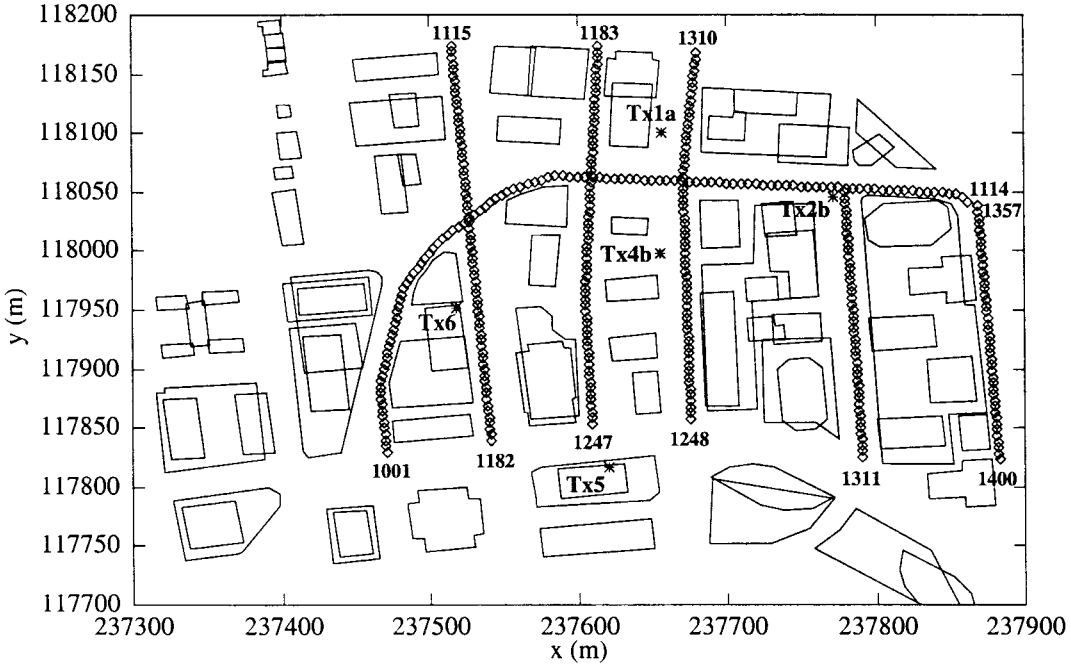

Fig. 7. Transmitter and receiver locations for core Rosslyn.

to the receiver. In conjunction with this path directly over the buildings, there can also be rays that reflect from a building wall in the vicinity of the source before propagating over the buildings and rays that reflect from a building wall near the receiver after the ray has gone over the other buildings. Finally, paths that undergo a single diffraction at a vertical corner of a building in combination with propagation over lower buildings or reflections will also contribute to the total power received at the receiver.

The SP/VP method, as described in [5], is intended to account for the paths that propagate over as well as around the buildings by confining the rays to lie in a set of orthogonal planes that contain the transmitter and receiver. This approximation can accurately predict the path loss if the difference in height between the transmitter and the receiver is not very large, and if the buildings are of nearly uniform height. On the other hand, for a rooftop transmitter, the slant plane becomes very steep and cannot properly account for ray paths that do not lie in this plane. For example, any ray that undergoes more than one reflection does not lie in the slant plane. An additional deficiency associated with a very steep slant plane occurs when the slant plane fails to intersect with the buildings that are further from the transmitter than the receiver. In this case, it is possible that a ray path can interact with those buildings before illuminating the receiver.

The VPL method overcomes the limitations of the SP/VP method because it allows the ray path between the source and receiver to lie anywhere in 3-D space. Although the actual ray tracing is confined to the vertical plane, the process of unfolding the all the vertical plane segments when resolving the vertical displacements allows the rays to travel any path in 3-D space. The only approximation to the ray path in the VPL method is that the rays diffracted at a horizontal edge are taken to lie in the incident and specularly reflected vertical planes instead of the diffraction cone of rays [1]. This approximation introduces a small error to the ray trace since the ray that arrives at a receiver is not completely contained within the unfolded vertical plane segments.

Predictions for the rooftop antenna were made with both the VPL and SP/VP methods. Fig. 8 compares the predictions of the VPL method (dashed curve), the SP/VP method (dotted curve), and the measurements (solid curve) for $Tx5$. The thick vertical lines separates the receivers along different streets of the measurement area. The VPL method is seen to provide better agreement with the measurements compared with the SP/VP method, especially for receivers close to the transmitter (receiver numbers 1155–1182 and 1315–1325). For these locations the SP/VP method misses some important rays reflected from the buildings because those rays are not confined to either the slant or vertical planes. The VPL method, however, can account for rays that propagate over buildings in addition to reflecting off a nearby building close to the transmitter or the receiver.

There is also a considerable improvement in computational time of the VPL method over the SP/VP method since only a single ray-trace set needs to be performed for the entire set of receivers in the VPL method. On the other hand, a separate ray tracing must be done for each distinct set of slant and vertical planes between each transmitter and receiver in the SP/VP method. In general, the VPL method is able to properly account for the ray paths for a rooftop antenna with substantially better run-time performance than the SP/VP method.

B. Comparison with the 2-D Method

For street-level transmitters that are 10 m above the ground, the predictions for the VPL and 2-D ray trace in the horizontal plane are expected to be similar when the surrounding

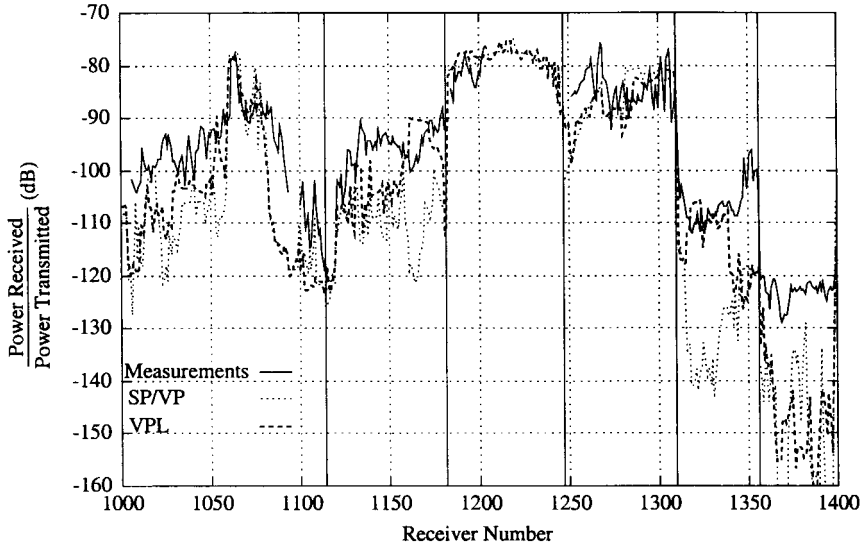

Fig. 8. Comparison of VPL and SP/VP methods versus measurements of rooftop antenna at 900 MHz.

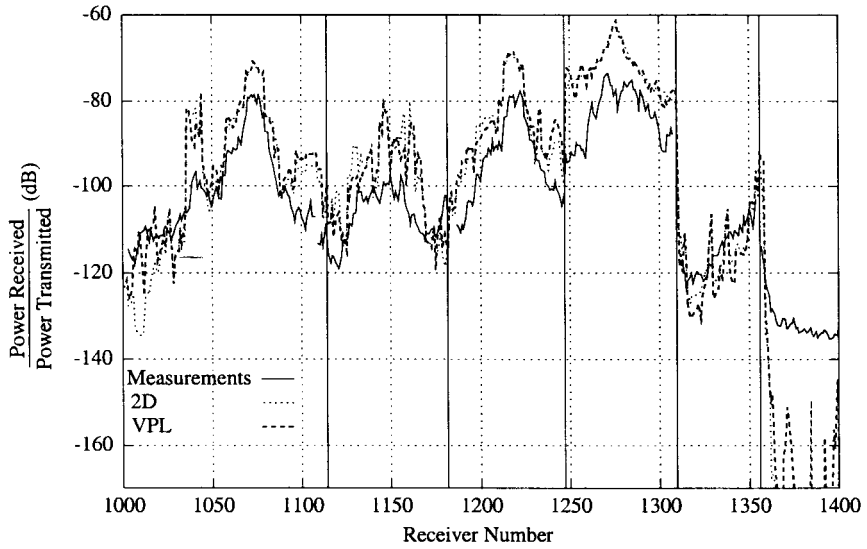

Fig. 9. Comparison of VPL and 2-D methods versus measurements for street level at 1900 MHz.

buildings are much higher. In a high-rise urban environment, propagation over the buildings does not significantly contribute to the total power received. Instead, the dominate propagation paths are expected to lie in a nearly horizontal plane that contains the transmitter and all the receivers. Therefore, the propagation mechanisms are associated with specular reflections from the walls, in combination with single or double diffraction at the vertical corners of the buildings. These ray paths can be accurately and readily found by performing a 2-D ray trace in the horizontal plane.

For an environment containing buildings of mixed height where not all the buildings are significantly higher than the source or the receiver, propagation paths that go over as well as around the buildings are needed for some receiver locations. In these cases, the 2-D ray trace provides pessimistic predictions. On the other hand, the VPL method retains the rays propagating over the buildings by accounting for the vertical dimension within the ray trace.

Fig. 9 shows a comparison of the predictions obtained from a 2-D ray trace (dotted curve), the VPL method (dashed curve), and the measurements (solid curve) for $Tx4b$, which is located near the center of core Rosslyn (shown in Fig. 7). The predictions for both methods were made by allowing one corner diffraction and up to six reflections before and after the corner diffraction. In combination with this, the VPL also includes a maximum of up to four diffraction at the horizontal building edges. In general, the predictions for both methods are more optimistic than the measurements, especially along the line of sight streets. On the other hand, along streets that are heavily shadowed from the transmitter, the 2-D method is very pessimistic while the VPL method provides closer agreement with the measurements. This is particularly evident for the receivers located on streets that are on the extreme left and right margins of the measurements areas (receiver locations 1001–1021 and 1357–1400). For receiver locations 1001–1021, the 2-D method provides slightly pessimistic pre-

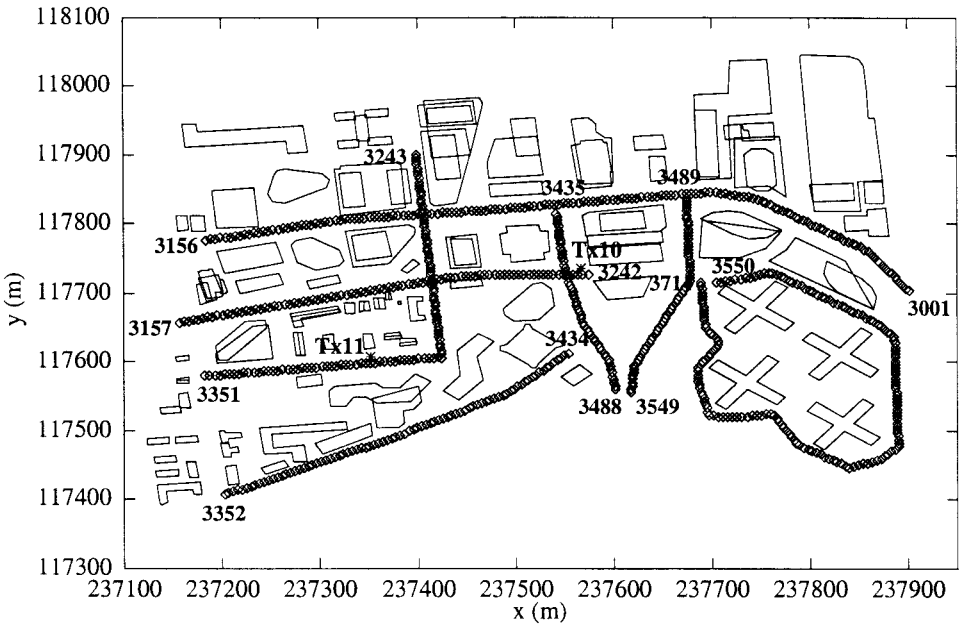

Fig. 10. Transmitter and receiver locations for south Rosslyn.

TABLE I
SUMMARY OF THE PREDICTION ACCURACY FOR COMPARISON BETWEEN METHODS

	900MHz					1900MHz			
	Tx 4b		Tx 5			Tx 4b		Tx 5	
	2D	VPL	VP/SP	VPL		2D	VPL	VPL	
η (dB)	4.72	6.05	-12.31	-5.40	η (dB)	5.52	6.05	-0.44	
σ (dB)	7.77	7.58	12.63	7.66	σ (dB)	8.30	7.65	7.06	

dictions while the predictions from the VPL method matches more closely with the measurements. On the other side of the prediction area at locations 1359–1400, due to heavy shadowing the 2-D prediction are so weak that they fall below the bottom limit of the graph. On the other hand, the VPL method still gives pessimistic predictions although they are now within 20 dB of the measurements.

In general, the VPL method is able to provide better results than the 2-D method for a mixed-height building environment such as it exist in Rosslyn. This improved result is due to the VPL method's ability to account for rays that propagate over the buildings that are not considered in the 2-D method. The cost is the increase in the computational time due to the additional complexity of considering rooftop diffraction.

In order to provide a quantitative assessment of the accuracy of each method, the average (η) and standard deviation (σ) of the prediction error is calculated for the difference between the predictions and measurements. The average error is used to show the systematic error of the prediction method, while the standard deviation of the error is intended to show the range of variation which would indicate the accuracy of the predictions. Table I shows the prediction errors for the VPL method and the other two methods for both frequencies. For all transmitter locations, the comparisons do not include the results for the receivers along Arlington Ridge Road (receiver locations 1357–1400) because the building database did not include a chain-linked fence lining the far side of the street which would have been a significant scatterer. The VPL is able to reduce the large variabilities of the other methods as reflected in the smaller value of σ. For $Tx4b$, η is larger for the VPL method because it does not give the very pessimistic prediction of the 2-D method at locations 1359–1400, which offset the generally optimistic predictions of both methods. For $Tx5$, the VPL method gives significantly smaller average error and standard deviation.

C. Comparison with Measurements for Other Tx Locations

Other sets of measurements were conducted in core Rosslyn for three additional transmitters locations ($Tx1a$, $Tx2b$, and $Tx6$) shown in Fig. 7, as well as for two other transmitters ($Tx10$ and $Tx11$) located 10 m above street level in a region that is shown in Fig. 10 south of the core area. The buildings within this area are similar to those in core Rosslyn, except in the region located at the bottom left-hand third of the map, where there are mainly low-rise residential buildings. Within this region there are 714 receivers locations numbered consecutively along each street, as shown in Fig. 10, that are 5 m apart and 2.5 m above the ground. There is also considerable terrain variation along both the x and y axes within this south Rosslyn area.

For $Tx10$ in south Rosslyn, the predictions at most locations are in good agreement with the measurements, as shown in Fig. 11. The predictions follows the major trends of the measurements for all streets except for receiver locations between 3352–3416 and 3598–3663 were they are 10–20 dB below the measurements. For these receivers the pessimistic predictions of VPL method result because we have allowed for only one diffraction from a vertical edge. When compared with the 2-D ray trace where double diffraction at vertical edges is included, it is evident that two vertical edge diffractions need to be accounted for in order to narrow the difference. The need to include double vertical edge diffraction is also evident for $Tx11$, as shown in Fig. 12, where predictions for the receivers

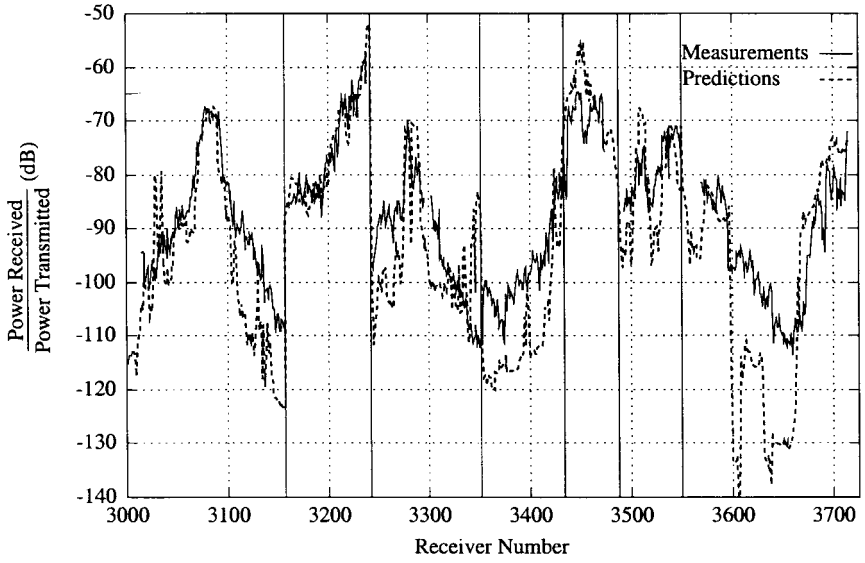

Fig. 11. Comparison of prediction versus measurements for $Tx10$ at 900 MHz.

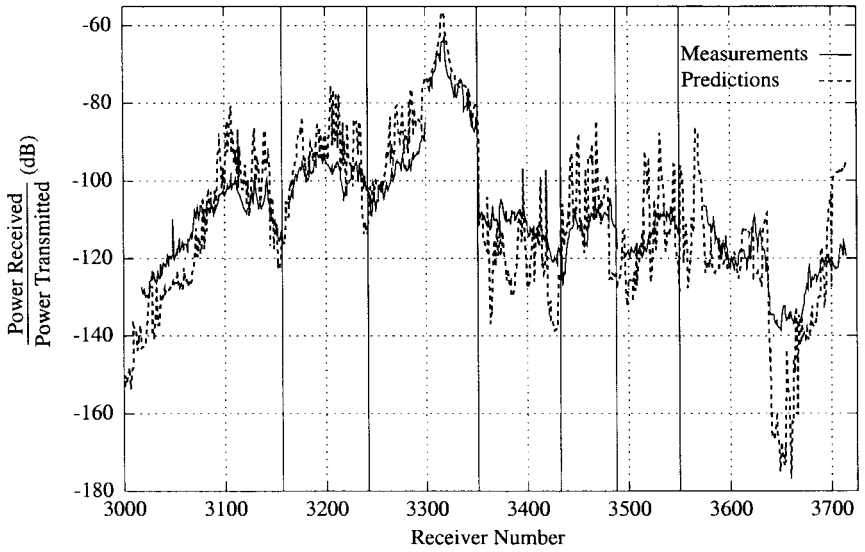

Fig. 12. Comparison of prediction versus measurements for $Tx11$ at 1900 MHz.

TABLE II
SUMMARY OF THE PREDICTION ACCURACY FOR VARIOUS OTHER Tx LOCATIONS

	900MHz		1900MHz	
	η (dB)	σ (dB)	η (dB)	σ (dB)
Tx 1a	-1.40	10.03	-4.19	10.10
Tx 2b	3.41	9.01	2.90	9.34
Tx 6	-8.44	5.92	2.79	6.14
Tx 10	-5.03	10.67	-3.84	11.84
Tx 11	0.11	10.52	-0.51	11.33

TABLE III
AVERAGE STATISTICAL RESULTS FOR BOTH TYPES OF TRANSMITTING ANTENNAS

	900MHz		1900MHz	
Tx	η (dB)	σ (dB)	η (dB)	σ (dB)
Street Level	2.35	9.22	2.28	9.88
Rooftop	-7.23	6.80	0.97	6.91

located in the deep shadows are more pessimistic than the overall predictions.

Table II lists the prediction errors for the rooftop and street-level antennas in core Rosslyn and the two 10-m base stations in south Rosslyn. As in the previous cases, the prediction errors for transmitters in core Rosslyn were calculated without the results for the receivers along Arlington Ridge Road (rx 1357–1400). In all cases, the predictions are on average more pessimistic than the measurements, primarily as a result of some receiver locations where the predictions are very low. In these regions it is necessary to account for rays that undergo double diffraction at vertical edges, especially for street-level antennas.

IV. CONCLUSION

The VPL method is a robust ray-tracing technique that can provide relatively accurate site specific propagation predictions in a heterogeneous building environment of a city for base-

station antennas located at various heights above the ground. The VPL is able to include a larger class of rays than the simpler 2-D ray trace in the horizontal plane, or the SP/VP method where the rays are confined to the slant and vertical planes between the transmitter and receiver. The method is able to overcome the deficiencies of the other methods without restoring to the complexity of a full 3-D ray trace. The ability to find the 3-D ray paths is particularly necessary for receiver points that are in the nonLOS regions where the propagation mechanisms into the regions are not intuitively obvious.

The model was validated with a large number of measurements for both rooftop and street-level transmitters in various locations of Rosslyn, VA. For each transmitter site, the average (η) and the standard deviation (σ) of the difference between the predictions and the measurements were calculated. In order to obtain an overall sense of accuracy for the VPL method, the weighted averages of η and σ for all the street level and rooftop antennas at both frequencies were computed and are listed in Table III. Table III indicates that the VPL method is able to provide predictions that have an average difference of about 2 dB for street level antenna and a standard deviation of approximately 9 dB at both 900 and 1900 MHz. For rooftop antennas, Table III show a larger systematic error associated with the 900 MHz results while a standard deviation of about 7 dB is obtained for both frequencies. In general, the results listed in Table III are very good in comparison to other theoretical and empirical methods used for site specific propagation predictions. Further improvements can be expected from the VPL technique by making the prediction with double vertical-edge diffraction for low base station and the inclusion of a more accurate model for terrain effects.

ACKNOWLEDGMENT

The authors would like to thank the Wireless Communications Systems Engineering Group of AT&T Holmdel, NJ, for providing us with the measurements.

REFERENCES

[1] J. B. Keller, "Geometrical theory of diffraction," *J. Opt. Soc. Amer.*, vol. 52, no. 2, pp. 116–130, Feb. 1962.
[2] L. R. Maciel, H. L. Bertoni, and H. H. Xia, "Unified approach to prediction of propagation over buildings for all ranges of base station antenna height," *IEEE Trans. Veh. Technol.*, vol. 42, pp. 41–45, Feb. 1993.
[3] K. Rizk, A. Mawira, J.-F. Wagen, and F. Gardiol, "Propagation in urban microcells with high rise buildings," in *IEEE VTS 46th Veh. Technol. Conf.*, Atlanta, GA, Apr. 1996, pp. 859–863.
[4] S. Y. Tan and H. S. Tan, "Propagation model microcellular communications applied to path loss measurements in Ottawa city streets," *IEEE Trans. Veh. Technol.*, vol. 44, pp. 313–317, May 1995.
[5] T. Kürner, D. J. Cichon, and W. Wiesbeck, "Concepts and results for 3-D digital Terrain-based wave propagation models: An overview," *IEEE J. Select. Areas Commun.*, vol. 11, pp. 1002–1012, Sept. 1993.
[6] W. Honcharenko, H. L. Bertoni, J. L. Dailing, J. Qian, and H. O. Yee, "Mechanisms governing UHF propagation on single floors in modern office buildings," *IEEE Trans. Veh. Technol.*, vol. 41, pp. 496–504, Nov. 1992.
[7] C. A. Balanis, *Advanced Engineering Electromagnetics.* New York: Wiley, 1989.
[8] O. Landron, M. J. Feuerstein, and T. S. Rappaport, "A comparison of theoretical and empirical reflection coefficients for typical exterior wall surfaces in mobile radio environment," *IEEE Trans. Antennas Propagat.*, vol. 44, pp. 341–351, Mar. 1996.
[9] L. B. Felsen and N. Marcuvitz, *Radiation and Scattering of Waves*. Englewood Cliffs, NJ: Prentice-Hall, 1973.
[10] R. F. Kouyoumjian and P. H. Pathak, "A uniform geometrical theory of diffraction for an edge in a perfectly conducting surface," *Proc. IEEE*, vol. 62, pp. 1448–1461, Nov. 1974.
[11] R. J. Luebbers, "Finite conductivity uniform GTD versus knife edge diffraction in prediction of propagation path loss," *IEEE Trans. Antennas Propagat.*, vol. AP-32, pp. 70–76, Jan. 1984.
[12] L. E. Vogler, "An attenuation function for multiple knife-edge diffraction," *Radio Sci.*, vol. 17, no. 6, pp. 1541–1546, Nov./Dec. 1982.
[13] J. Walfisch and H. L. Bertoni, "A theoretical model of UHF propagation in urban environments," *IEEE Trans. Antennas Propagat.*, vol. 36, pp. 1788–1796, Dec. 1988.
[14] H. H. Xia and H. L. Bertoni, "Diffraction of cylindrical and plane waves by an array of absorbing half-screens," *IEEE Trans. Antennas Propagat.*, vol. 40, pp. 170–177, Feb. 1992.
[15] W. C. Y. Lee, *Mobile Communications Engineering*, 1st ed. New York: McGraw-Hill, 1982.
[16] H. L. Bertoni, W. Honcharenko, L. R. Maciel, and H. H. Xia, "UHF propagation prediction for wireless personal communications," *Proc. IEEE*, vol. 82, pp. 1333–1359, Sept. 1994.

George Liang (S'89–M'91–S'95–M'98) was born in Hong Kong on March 6, 1968. He received the B.S. degree in electrical engineering from the University of British Columbia, Vancouver, Canada, in 1991, and the M.S. (in electrophysics) and Ph.D. degrees (electrical engineering) both from Polytechnic University, Brooklyn, NY, in 1995 and 1997, respectively.

From 1991 to 1994, he was employed at Timber Hill, Inc., Valhalla, NY, as an Network Engineer. In 1994 he joined the propagation prediction group at Polytechnic University as a Research Assistant. Since 1997 he has been the President and Principle Researcher at Site Ware Technologies, Inc., a high technology research firm that he co-founded. The focus of his work involves the development of a full-function propagation prediction software tool for mobile and wireless communications.

Henry L. Bertoni, (M'67–SM'79–F'87) was born in Chicago, IL, on November 15, 1938. He received the B.S. degree in electrical engineering from Northwestern University, Evanston, IL, in 1960, and the M.S. (electrical engineering) and Ph.D. degrees (electrophysics) from the Polytechnic Institute of Brooklyn (now Polytechnic University), Brooklyn, NY, in 1962 and 1967, respectively.

After graduation he joined the faculty of the Polytechnic Institute of Brooklyn, eventually becoming Head of the Electrical Engineering Department (1990–1995), and serving as Vice Provost of Graduate Studies (1995–1996). His research has dealt with theoretical aspects of wave phenomena in electromagnetics, ultrasonics, acoustics, and optics. He has authored or coauthored over 110 journal and proceedings papers on these topics. From 1982 to 1983 he spent a sabbatical leave at University College, London, U.K., as a Guest Research Fellow of the Royal Society. During the summer of 1983 held a Faculty Research Fellowship at USAF Rome Air Development Center, Hanscom AFB, OH. His current research in electromagnetics deals with the theoretical prediction of UHF propagation characteristics in urban environments.

Dr. Bertoni was the first Chairman of the Technical Committee on Personal Communications of the IEEE Communications Society and was IEEE representative to and chairman of the Hoover Medal Board of Award. He has served on the ADCOM of the IEEE Ultrasonics, Ferroelectric, and Frequency Control Society. He is also a member of the International Scientific Radio Union and the New York Academy of Science. He was awarded the 1984 Best Paper Award of the IEEE Sonics and Ultrasonics Group and the 1993 Neal Shepherd Best Propagation Paper Award of the IEEE Vehicular Technology Society.